

# SOFTWARE PACKAGE FOR DEM ESTIMATION USING SAR INTERFEROMETRY

Kirti Padia, P. Robert and S. K. Basu  
Image Processing and Data Products Group  
Space Applications Centre (ISRO),  
Ahmedabad - 380 053.  
Gujarat, India

Commission I, Working Group 3.

**KEY WORDS :** Interferometric SAR , DEM, Baseline, SLC, AFF, Phase unwrapping , GCP

## ABSTRACT

Interferometric SAR (InSAR) is a technique to derive topographic information by exploiting the phase information obtained from multiple pass satellite data or in a single pass with two antennas. Topographic information can be used to derive slope maps and surface change detection. In InSAR, the same point on the ground is viewed by two antennas separated by some distance. This type of viewing geometry causes a path difference, which results in phase difference. This phase is due to topography and due to change in back scattering conditions of target. If the time period between the two acquisitions is small then phase change due to terrain change can be neglected and knowing the geometry accurately, we can obtain information about topography. This paper describes the methodology adopted and details about the software developed. From the DEM generated, height values of few GCPs (Ground Control Point) are compared with height values from topographic maps. RMS accuracy of better than 10 meters was achieved over 24 x 24 Km. area of moderately hilly region.

## 1. INTRODUCTION

Synthetic Aperture Radar (SAR) is a coherent microwave imaging system. High resolution images are obtained using the motion of the sensor platform and synthesizing a long aperture antenna from a physically small antenna. The terrain points are placed on the two dimensional SAR image according to their slant range to sensor and their relative along track positions. Topographic information is obtained from the phase difference of two single look complex (SLC) images and viewing geometry of area of interest (Fig. 1). To obtain the phase difference, the two SLC need to be registered at sub-pixel level. Phase in the interferogram obtained after registering the two SLC images, vary modulo  $2\pi$  (i.e.  $-\pi$  to  $\pi$ ). This is known as principle phase. To obtain height at a given point, it is required to know the absolute phase at that point. This is obtained by unwrapping the phase after removing the phase due to viewing geometry. Also, orbit information available with the scene may not be oftenly accurate enough so it need to be refined using GCPs and unwrapped phase. The details of methodology adopted and software developed on DEC-Alpha system using FORTRAN-90 and C languages and OSF environment is discussed in the subsequent sections.

## 2. INSAR BASICS

Consider an InSAR viewing geometry shown in Fig.(1). The same point on the ground is viewed by two antennas  $A_1$  and  $A_2$  separated by a distance known as baseline  $B$ . Let slant range values corresponding to this viewing geometry are  $R_1$  and  $(R_1 + \delta)$ . This path difference  $\delta$  in slant range creates a phase difference  $\phi$  which can be expressed as

$$\phi = (4\pi / \lambda) * \delta \quad (1)$$

From the viewing geometry, the following relation can be deduced.

$$(R_1 + \delta)^2 = R_1^2 + B^2 + 2 R_1 B \sin(\alpha - \theta) \quad (2)$$

Where  $\alpha$  is baseline orientation angle and  $\theta$  is look angle.

The height  $Z$ , of a target is obtained from

$$Z = H - R_1 \cos \theta \quad (3)$$

Where  $H$  is height of satellite.

The phase difference  $\phi$  obtained from two SAR SLC images by conjugate complex multiplication is expressed as

$$D_n = D_{I_n} + D_{Q_n} = |A_n| e^{j\phi_n} \quad (4)$$

### 3. METHOD

#### 3.1 Manual Registering of Images

The input SLC images are first detected and displayed on the screen. From the display course registration (up to a pixel level) is obtained between the two SLC data set. This information is used for sub-pixel registration of the two SLC data set.

#### 3.2 Sub-Pixel Registration and Fringe Generation

From the two SLC data set, one data set is chosen as a fixed image and other data set is interpolated to 1/10 th of a pixel. Over a fixed window size, phase difference is obtained between fixed and interpolated image. The Average Fluctuation Function (AFF) of the phase difference is computed for each pixel (Lin, 1992). Exact registration corresponds to the minimum value of AFF. The AFF is computed as

$$f = \left( \sum_i \sum_j |P(i+1, j) - P(i, j)| + |P(i, j+1) - P(i, j)| \right) / 2 \quad (5)$$

Where  $P(i, j)$  is phase difference corresponding to  $(i, j)$  th location. Using orbit information baseline estimation is done and phase due to flat earth earth is removed from the interferogram.

#### 3.3 Noise Filtering

The interferogram generated after registering two SLC is smoothened by doing filtering. In the filtering process, each sample in a window is assumed as a vector. The value of central vector is replaced by average of the surrounding vectors (Padia, 1997).

#### 3.4 Phase Unwrapping

The interferogram obtained after registration, flat earth correction and filtering will have values between  $-\pi$  and  $\pi$ . This phase information needs to be unwrapped before it is used to derive height information at a point. Layover, shadow and noise are characteristics of SAR imaging. They cause discontinuities in the phase. These discontinuities known as "residues" need to be avoided while performing unwrapping process, otherwise phase error

is propagated globally which results ultimately in wrong estimation of height (Hartle, 1993). Residue is identified by calculating sum of phase difference at a point in the interferogram. If this sum is  $+2\pi$  then it is called a positive residue and if sum is  $-2\pi$  then it is called a negative residue. The residue method adopted for unwrapping first finds positive and negative residues in the interferogram and nearest opposite residues are connected to form ghost lines. For unwrapping a pixel, path is chosen such that it does not cross any ghost line. Thus global propagation of phase error is avoided. A seed pixel location is provided to start the unwrapping process.

#### 3.5 Baseline Estimation

The baseline is defined as the cross orbit separation; i.e. the distance perpendicular to the satellite flight direction between two repeat orbits. Along with each SLC, ephemeris data containing satellite position and velocity information at a certain interval of time is available. For the reference scene, position and velocity information at a specified time is interpolated using a least square fit. The repeat orbit is then propagated iteratively till the optimum orbit separation is achieved (Padia, 1997). The accuracy of baseline by this method is limited to the accuracy of orbit information, which is not enough often. For better accuracy, ground control points (GCPs) are used. Using the unwrapped phase for selected gcps, and height values from topomap, following equation is solved using non linear least square method.

$$\sin(\alpha - \theta) = \lambda * (\phi + \phi_0) / (4\pi B) \quad (6)$$

Where  $\lambda$  is wavelength of SAR sensor,  $\phi_0$  is phase constant to take into account absolute phase. Baseline is modeled as cross track component  $B_c$  and normal component  $B_n$ .

$$B_c = B_{c0} + \mu t \quad (7)$$

$$B_n = B_{n0} + \nu t \quad (8)$$

$B_{c0}$  and  $B_{n0}$  are nominal values of baseline cross track and normal component respectively.

#### 3.6 Height and Slope Calculation

Using corrected baseline information, phase constant and eq. (3), height values are computed for each pixel. From the computed height values, slope is computed

as change in height with distance and is shown as percentage slope in slope image. Using geometry and ephemeris information, slant plane height and slope values are converted to ground plane.

#### 4. SOFTWARE OVERVIEW

Using the above mentioned methodology, software has been developed on DEC-Alpha system using FORTRAN-90 and C language. Software flow diagram is shown in Fig.(2). Software generates height and slope information at 40 x 40 meters interval. Major inputs required are SLC data pair and corresponding ephemeris information, pixel level registration information in terms of scanline and pixel location in both SLC data set, few GCPs(more than 5) in the area of interest and location of seed pixel to start unwrapping. Execution of all modules is done through a driver routine.

#### 5. TEST RESULTS

Using the software DEM generation was performed for two data sets of ERS-1 and ERS-2 SAR SLC data. Survey of India topomaps of 1:25000 scale were used for identification of GCPs. From the GCPs selected for each data set, few were used to refine the baseline estimation and phase constant evaluation and rest were used as check points. Details of results obtained for each test data is as follows :

##### Data set 1

Path : 698 Row : 199  
 Size of area : 20.5 x 20.5 Km.  
 ERS-1 date of pass : 23-4-96  
 ERS-2 date of pass : 24-4-96

##### Data set 2

Path : 756 Row : 194  
 Size of area : 24.0 x 24.0 Km.  
 ERS-1 date of pass : 11-4-96  
 ERS-2 date of pass : 12-4-96

Table 1 shows the baseline estimation using ephemeris data and using GCPs information. Table 2 shows information about GCPs used to refine baseline information and error in their heights. Table 3 shows error in height estimation for GCPs used as check points. Fig. (3) shows a typical SLC (10 x 2) averaged image and Fig. (4) is an interferogram corresponding to the same area after flat earth correction and filtering. Fig. (5) and (6) show height image and slope image respectively, corresponding to interferogram of Fig. (4).

#### 6. CONCLUSION

Software has been developed to generate DEM from a pair of SAR SLC data. First cut verification results using Survey of India topomaps are encouraging. Software works well when terrain is moderately hilly. Detailed verification need precise measurement of GCPs using GPS measurements, which is being planned.

#### 7. REFERENCES

- Hartle P. and Wu X., 1993. SAR interferometry experiences with various phase unwrapping methods. Proc. Second ERS-1 symp., Space at the service of our Environment.
- Lin Q., Vesecky J. F. and Zebkar H. A., 1992. New approaches in interferometric SAR data processing. IEEE trans. On Geo. Sci. and Rem. Sensing, Vol. 30,no.3,May.
- Padia K., Robert P. and Basu S. K., 1997. Software package for height estimation using SAR interferometry. /SAC/IPDPG/TN-01/JUNE .

	Data set	Baseline parallel component	Baseline perpendicular component	Baseline
Using Ephemeris data	Data set 1	-54.908	-107.347	120.575
	Data set 2	-49.356	-101.125	112.528
Using GCPs	Data set 1	-55.015	-108.350	121.517
	Data set 2	-46.611	-85.327	97.229

Table 1: Baseline estimation using ephemeris data and GCPs.

Sr. No.	Scan No.	Pixel No.	Height from Map	Height Using Software	Difference Soft. - Map
1.1	379	443	40.00	29.221	-10.779
1.2	506	330	69.00	68.643	-0.357
1.3	205	330	40.00	45.725	5.725
1.4	345	121	67.00	70.617	10.617
1.5	91	474	100.00	95.322	-4.678
2.1	408	324	235.00	237.593	2.593
2.2	520	506	293.00	289.013	-3.987
2.3	17	70	200.00	192.847	-7.153
2.4	84	513	205.00	210.320	5.320
2.5	250	70	210.00	213.00	3.000

Table 2: GCPs used to refine baseline information and error in their heights after baseline refinement

Sr. No.	Scan No.	Pixel No.	Height from Map	Height Using Software	Difference Soft. - Map
1.1	437	444	42.00	39.280	-2.720
1.2	400	497	30.00	24.365	-5.635
1.3	300	67	590.00	588.079	-1.921
1.4	372	187	190.00	184.323	-5.677
1.5	76	462	105.00	105.472	0.472
2.1	360	288	223.00	226.840	3.840
2.2	460	504	221.00	216.798	-4.202
2.3	171	204	203.00	205.348	2.348
2.4	181	495	203.00	206.098	3.098

Table 3: GCPs used as check points and error in their heights

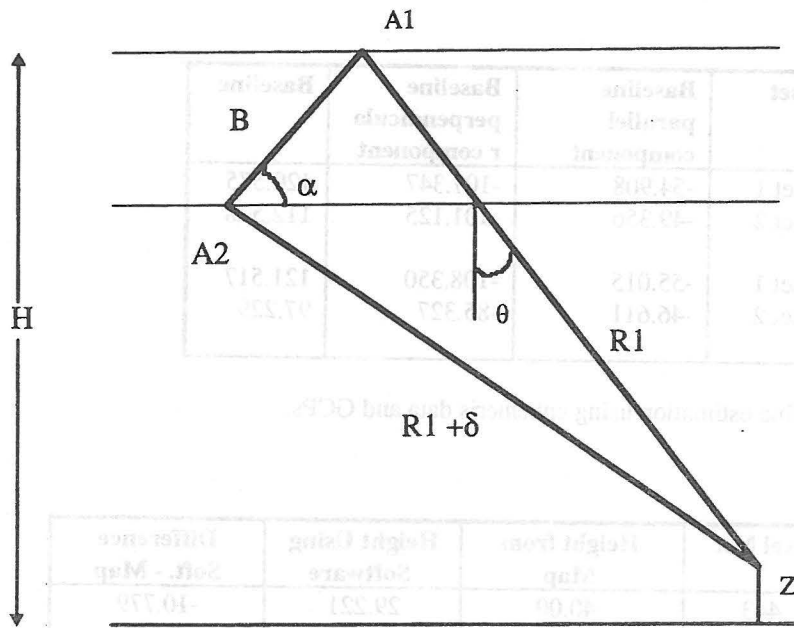


Fig. 1 Viewing Geometry

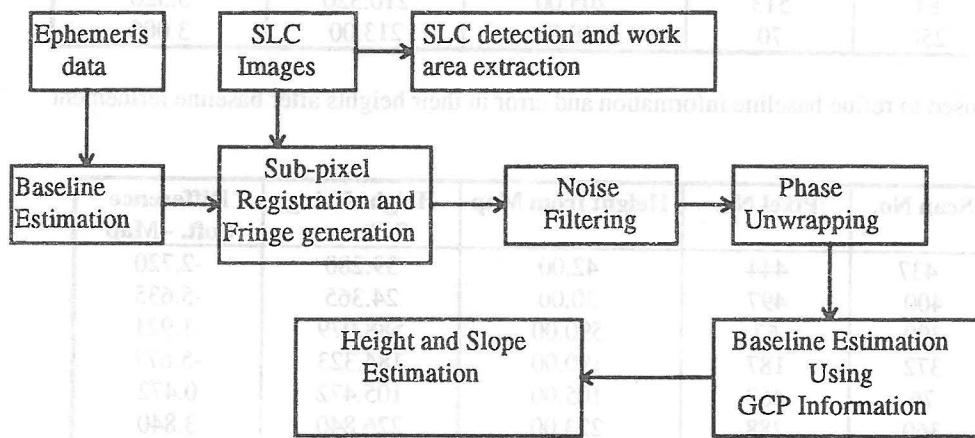


Fig. 2 Block diagram showing functioning of InSAR software

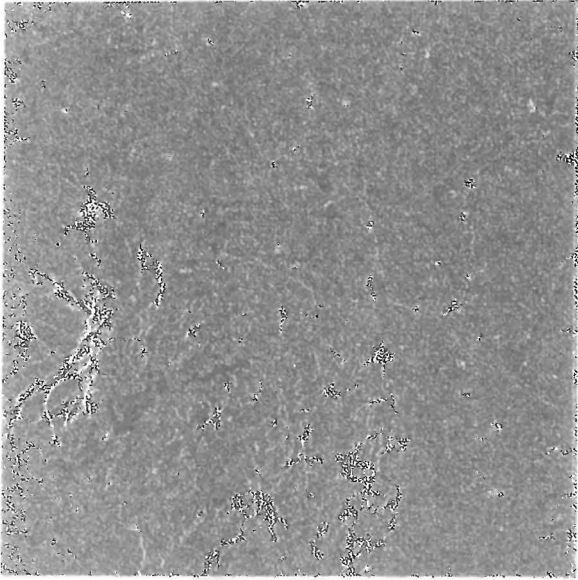


Fig. 3 A (10 x 2) averaged SAR SLC image

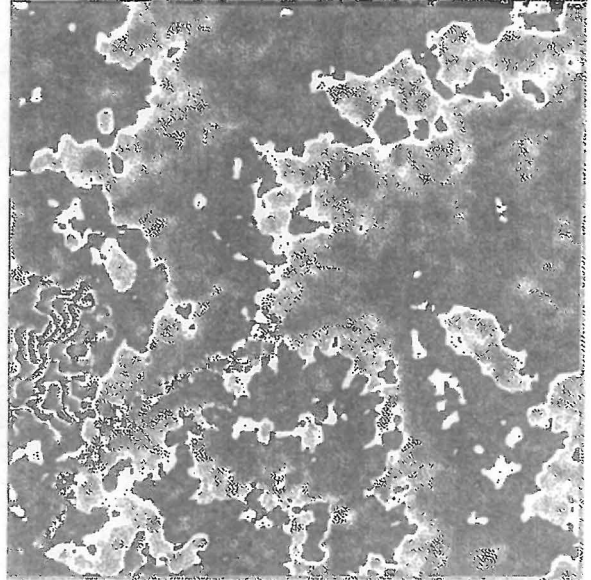


Fig. 4 Interferogram corresponding to image in Fig.(3)

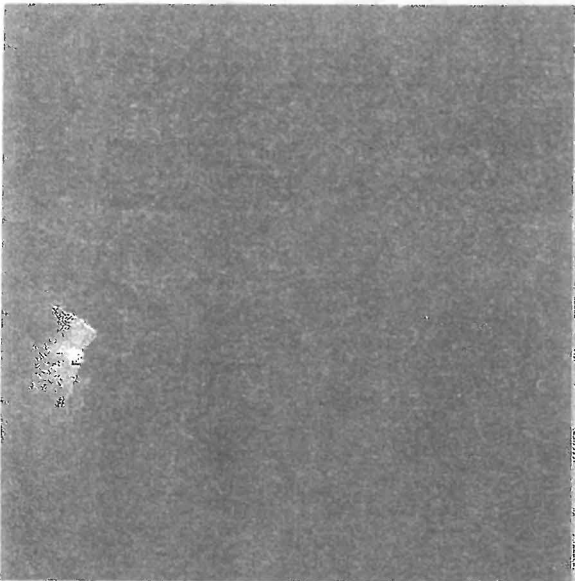


Fig. 5 Height image corresponding to image in Fig. (3)

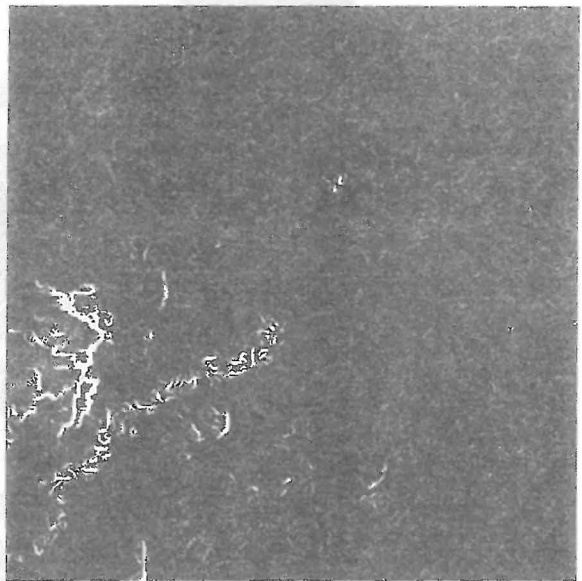


Fig. 6 Slope image corresponding to image in Fig. (3)

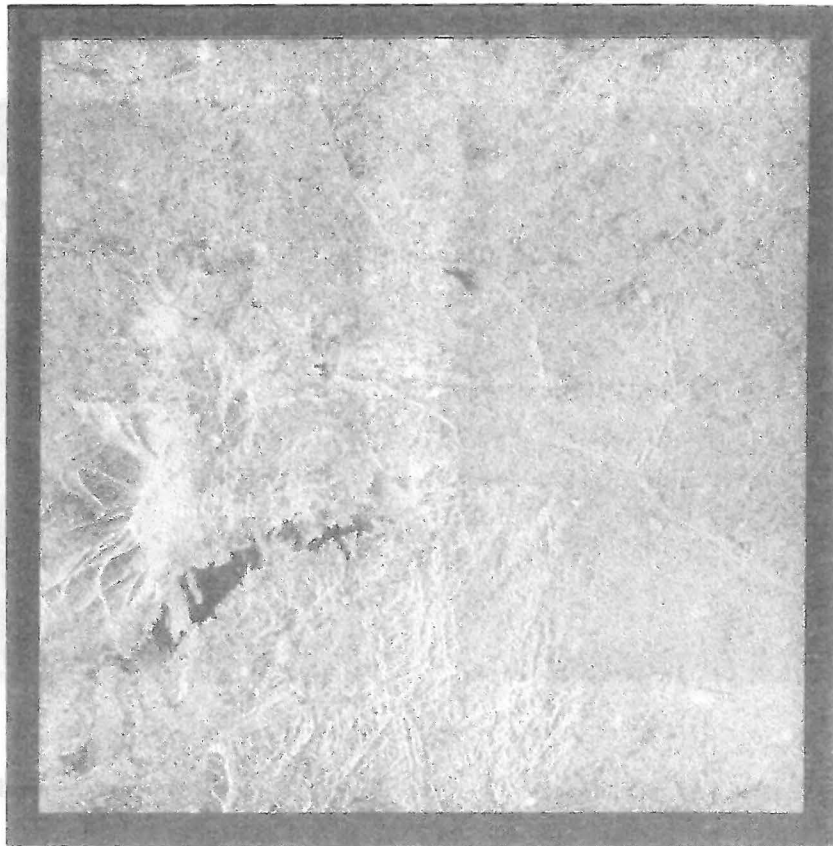


Fig. 3 A (10 x 2) averaged SAR SLC image

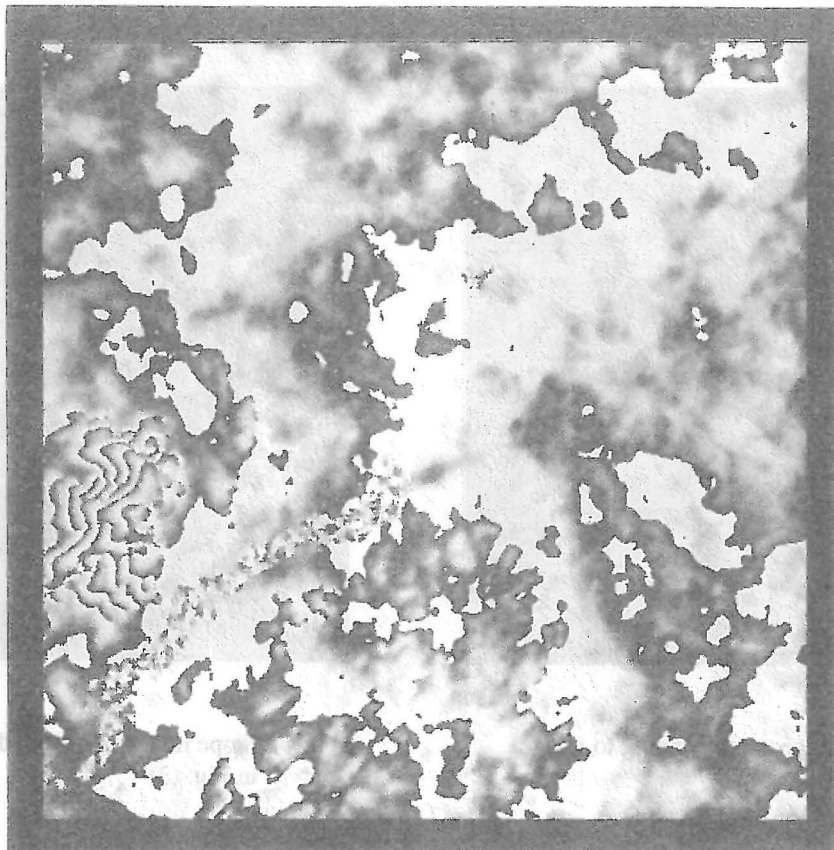


Fig. 4 Interferogram corresponding to image in Fig. (3)

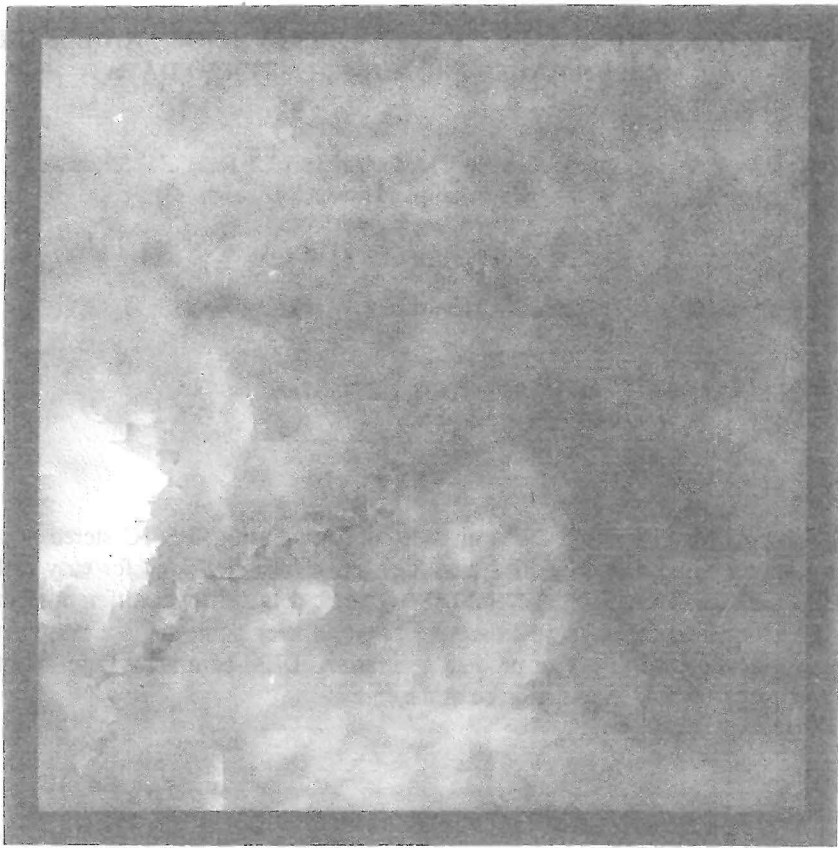


Fig. 5 Height image corresponding to image in Fig. (3)

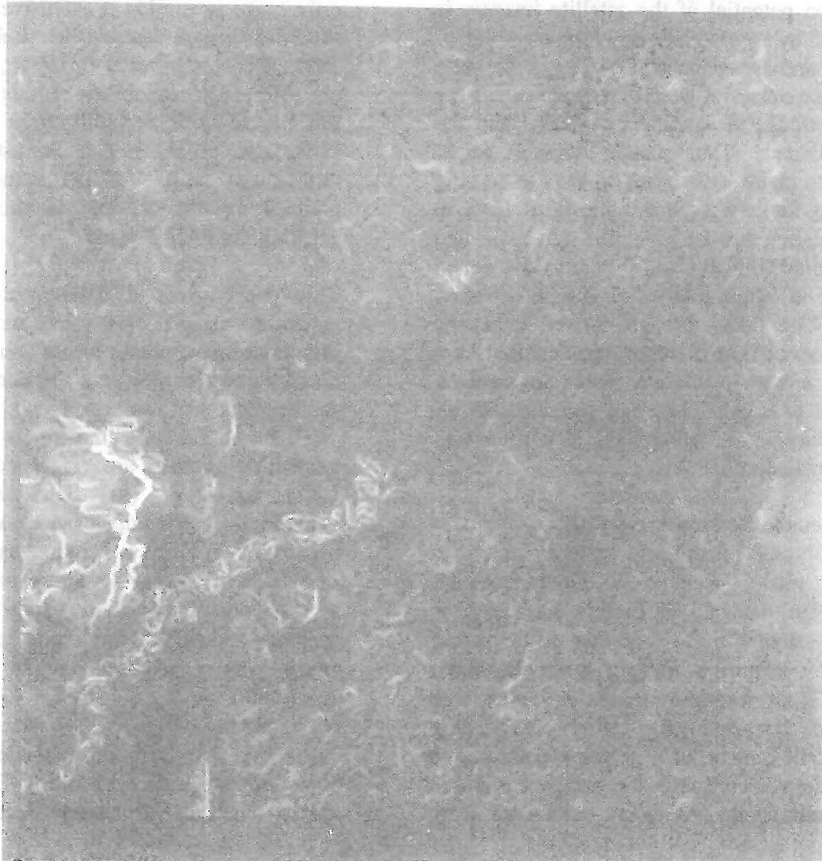


Fig. 6 Slope image corresponding to image in Fig. (3)